$$Fe^{II}TMP + NO_2^- = Fe^{III}TMP + NO_2^{2-} \quad \text{(rate-determining step)} \quad (13)$$

$$NO_2^{2-} + 2H^+ = H_2O + NO \text{ (fast)} \quad (14)$$

Nitrite attack is faster than nitrous acid attack because of electrostatic and stereochemical considerations. The dipositive charge on the complex favors interaction with anionic species. Nitrite has no hindered side, but HNO_2 cannot accomplish electron transfer through the side that possesses the proton. The inertness of the $Fe^{II}TMP$ coordination shell and the rapidity of the reaction imply that the electron transfer proceeds by an outer-sphere mechanism. Rates of reaction with nitrous acid are in the order $Cr(H_2O)_6^{2+} > Fe^{II}TMP > Fe(H_2O)_6^{2+}$. The hexaaquochromium(II) ion does not have the conjugated π system around the metal center to facilitate electron transfer as in $Fe^{II}TMP$. This lack is apparently compensated, however, by the substantially greater thermodynamic driving force in the chromium–nitrous acid system.

The hexaaquoiron(II)–nitric(ous) acid systems were found to be autocatalytic in the product NO. No evidence of autocatalysis has been found in the present system either in our experimental data or in the simulations. The autocatalytic sequence in the mechanism proposed for the hexaaquoiron system[2] consists of reactions P2, P3, and P7. Apparently, with $Fe^{II}TMP$ the NO_2 produced by (P7) reacts preferentially with the ferric species (which is formed much more rapidly than in the hexaaquo system) via (P1) rather than with $Fe^{II}TMP$ in (P2) as required for the development of autocatalysis.

In spite of limitations on interpretation of the experimental data and on the quantitative agreement between calculation and experiment for phase 2 of the reaction, the present study has provided considerable information about the $Fe^{II}TMP$–nitrous acid system. Rate constants for the reactions of the complex with nitrite and nitrous acid have been determined. A qualitative picture of the origin of the regeneration of the catalyst has been developed. Remarkable agreement has been obtained between the experimental results and those derived from a model for the hexaaquoiron(II)–nitric acid system with the introduction of only a single new adjustable parameter. This investigation also represents one of the first efforts at combining experimental kinetics techniques with numerical simulation to elucidate the nature of homogeneous catalysis.

Acknowledgment. We thank Dr. Irwin Taub for informative discussions. This work was supported by National Science Foundation Grant CHE 7905911 and by NIH Research Grant GM 08893-18.

Registry No. $Fe^{II}TMP$, 17378-70-0; HNO_2, 7782-77-6; NO_2^-, 14797-65-0.

Magnetic Exchange in Imidazolate-Bridged Copper(II) Complexes

Gary Kolks,[1a] Stephen J. Lippard,*[1a] Joseph V. Waszczak,[1b] and Henry R. Lilienthal[1c]

Contribution from the Department of Chemistry, Columbia University, New York, New York 10027, Bell Laboratories, Murray Hill, New Jersey 07974, and the Physical Sciences Department, T. J. Watson Research Center, Yorktown Heights, New York 10598. *Received July 6, 1981*

Abstract: Variable-temperature (4.2–300 K) magnetic susceptibility studies of a variety of imidazolate and substituted imidazolate-bridged dicopper(II) complexes reveal that the imidazolate (im) group can mediate moderate antiferromagnetic interactions. The observed coupling constants (J) for a series of tridentate amine copper(II) complexes in which the bridging ligands are imidazolate, 2-methylimidazolate, benzimidazolate, and 2-methylbenzimidazolate, −26.90 (2), −38.1 (3), −16.99 (1), and −29.82 (4) cm^{-1}, respectively, parallel the first pK_a values of the respective free imidazoles. This behavior is best accounted for by a σ-exchange pathway. Two coupling constants, −87.64 (4) and −35.0 (4) cm^{-1}, are required to fit the data for $[Cu_2(bpim)(im)]_2^{4+}$, a cation having two geometrically distinct imidazolate-bridged dicopper(II) units. Assignment of the coupling constants to their respective bridging imidazolate rings in this tetranuclear cation is achieved by comparison to the J values obtained for Cu_2bpim^{3+} and $[Cu(pip)]_2(im)^{3+}$ (bpim is 4,5-bis[((2-(2-pyridyl)ethyl)imino)methyl]imidazolate and pip is 2-[((2-(2-pyridyl)ethyl)imino)methyl]pyridine). The large negative J value observed for Cu_2bpim^{3+} is rationalized on the basis of the near collinearity of the Cu–N(imidazolate) bonds which increases the through-bond interaction of the nitrogen lone pair orbitals with each other and leads to increased antiferromagnetic coupling. These studies verify the existence of an imidazolate-bridged dicopper(II) center in a form of bovine erythrocyte superoxide dismutase in which Cu(II) replaces Zn(II) and provide a foundation for the identification of imidazolate (histidine) bridged centers in other metallobiomolecules.

Two or more paramagnetic metal atoms bridged by a common diamagnetic ligand may interact via electronic exchange coupling (superexchange) to exhibit overall ferromagnetic or antiferromagnetic behavior.[2-4] Although this behavior can result from metal–metal bonding, the large distance between metal centers (often 3 Å or greater) usually precludes direct overlap of the metal orbitals. In such cases the bridging ligand mediates the exchange interaction providing a pathway through which the metal orbitals can interact.

The exchange-split cluster energy levels are given[2] by the application of the Heisenberg–Dirac–Van Vleck spin-coupling Hamiltonian (eq 1), where J_{ab} is the exchange coupling constant

$$\hat{\mathcal{H}}_{ex} = -2\sum_{a,b} J_{ab}\hat{S}_a\cdot\hat{S}_b \quad (1)$$

for the interaction between metal atoms at sites a and b with total

(1) (a) Columbia University. (b) Bell Laboratories, Murray Hill. (c) IBM Yorktown Heights.
(2) Ginsberg, A. P. *Inorg. Chim. Acta Rev.* **1971**, *5*, 45.
(3) Martin, R. L. In "New Pathways in Inorganic Chemistry", Ebsworth, E. A. V., Maddock, A. G., Sharpe, A. G., eds.; Cambridge University Press: New York, 1968; Chapter 9.
(4) Hodgson, D. J. *Prog. Inorg. Chem.* **1975**, *19*, 173.

0002-7863/82/1504-0717$01.25/0

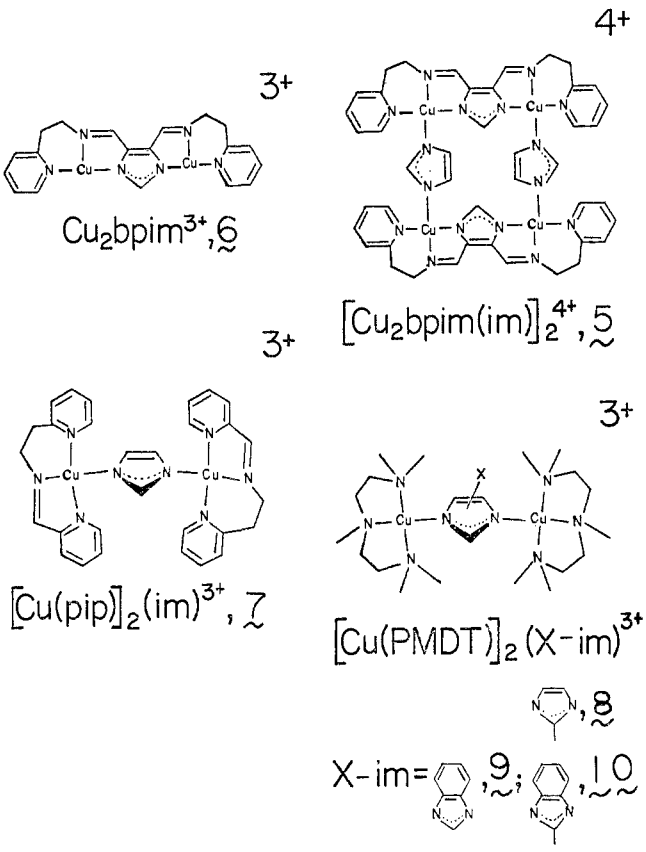

Figure 1. The imidazolate-bridged polynuclear copper(II) complexes discussed in this paper.

spin operators $\hat{S}_a$ and $\hat{S}_b$. Comparison of experimentally obtained variable-temperature magnetic susceptibility data with values calculated by application of eq 1 leads to the determination of J_{ab}. By convention, a negative value of J_{ab} indicates antiferromagnetic behavior and a positive value of J_{ab} ferromagnetic behavior.

The magnetic exchange properties of dimers of Cu(II)[4] or Cr(III)[5] bridged by hydroxide or halide ligands is understood on a semiquantitative level.[6] The results of these important studies may be used to rationalize the behavior of other systems containing monodentate bridging ligands. Such success has not been attained with polyatomic bridging ligands. It was suggested,[6] for example, that the σ electron systems of pyrazine, **1**, and diazabicyclooctane,

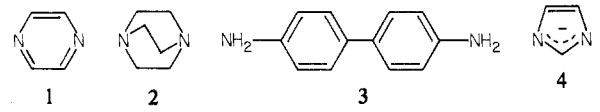

1 2 3 4

2, should promote reasonably large superexchange interactions. No exchange coupling is observed in Cu(II) dimers[7] containing **2**, however. Compounds with **1** as a bridging ligand exhibit[7] only very weak antiferromagnetic coupling which, in at least one series of well-studied compounds, has been ascribed to exchange interactions through the pyrazine π-electron system.[8] Inexplicably, the exchange coupling mediated by **3**[9] is comparable to that mediated by **1**, despite their different sizes.

This paper describes a systematic study of magnetic exchange interactions in a series of imidazolate (**4**) bridged polynuclear

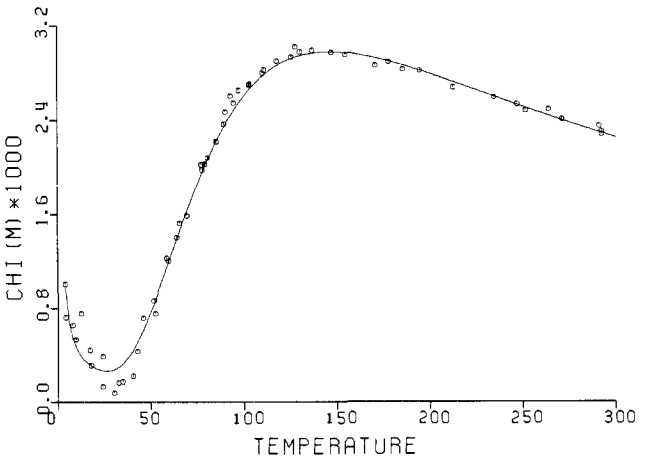

Figure 2. Corrected molar magnetic susceptibility ($cm^3\ mol^{-1}$) vs. absolute temperature for $[Cu_2(bpim)(NO_3)_2]ClO_4 \cdot 2H_2O$, **6**. Experimental data are shown as open circles. The solid line shows the least-squares fit to the data using the parameters and equations described in the text.

copper(II) complexes shown in Figure 1. As described in a preliminary report,[10] compound **5** contains two kinds of bridging imidazolate groups and two very different coupling constants are required to fit the magnetic susceptibility data.[11] The assignment of the coupling constants to the respective type of bridging ligand was possible[11] only after the synthesis and study of compounds **6** and **7** (Figure 1). As shown here, magnetic studies of **7**–**10** reveal that J_{ab} depends upon the basicity of the bridging imidazole. Moreover, since imidazolate-bridged bimetallic centers are known[12,13] or postulated[14] to occur in biological compounds, the present results should be helpful in identifying bridging histidine ligands in metallobiomolecules of unknown structure. They have already been employed by workers who question the presence of a bridging imidazolate group in cytochrome *c* oxidase.[15]

Experimental Section

The compounds $[Cu_2(bpim)(im)]_2(NO_3)_4 \cdot 4H_2O$, **5**, $[Cu_2(bpim)(NO_3)_2](ClO_4) \cdot 2H_2O$, **6**, $[Cu(pip)]_2(im)(NO_3) \cdot 2.5H_2O$, **7**, and $[Cu(PMDT)]_2(X\text{-im})(ClO_4)_3$ (X-im = 2-methylimidazolate, benzimidazolate, and 2-methylbenzimidazolate, **8**, **9**, and **10**, respectively) were prepared as described in the first paper of this series.[16] The structures of **5**–**9** have been determined by X-ray crystallography.[17]

Variable-temperature (4.2–300 K) magnetic susceptibility measurements were made on finely ground samples by using the Faraday method. Field strengths of 6–18 kOe were employed. Descriptions of the apparatus used appear in ref 18 and 19.

Corrections for the small amounts of saturated ferromagnetic impurities found in each compound were obtained by measuring the field dependence of the magnetic susceptibility and extrapolating to infinite field.[20] For compounds **6** and **8** this correction was determined at each temperature while for the remaining compounds the correction factor obtained at room temperature was used for all of the data.

(5) Cline, S. J.; Kallesøe, S.; Pederson, E.; Hodgson, D. J. *Inorg. Chem.* **1979**, *18*, 796.
(6) Hay, P. J.; Thibeault, J. C.; Hoffmann, R. *J. Am. Chem. Soc.* **1975**, *97*, 4884.
(7) Haddad, M. S.; Hendrickson, D. N.; Cannady, J. P.; Drago, R. S.; Bieksza, D. S. *J. Am. Chem. Soc.* **1979**, *101*, 898.
(8) Richardson, H. W.; Hatfield, W. E. *J. Am. Chem. Soc.* **1976**, *98*, 835.
(9) Felthouse, T. R.; Duesler, E. N.; Hendrickson, D. N. *J. Am. Chem. Soc.* **1978**, *100*, 618.
(10) Kolks, G.; Frihart, C. R.; Rabinowitz, H. N.; Lippard, S. J. *J. Am. Chem. Soc.* **1976**, *98*, 5720.
(11) Kolks, G.; Lippard, S. J. *J. Am. Chem. Soc.* **1977**, *99*, 5804.
(12) (a) Richardson, J. S.; Thomas, K. A.; Rubin, B. H.; Richardson, D. C. *Proc. Natl. Acad. Sci. U.S.A.* **1975**, *72*, 1349. (b) Beem, K. M.; Richardson, D. C.; Rajagopalan, R. V. *Biochemistry* **1977**, *16*, 1930.
(13) Fee, J. A.; Briggs, R. G. *Biochim. Biophys. Acta* **1975**, *400*, 439.
(14) (a) Palmer, G.; Babcock, G. T.; Vickery, L. E. *Proc. Natl. Acad. Sci. U.S.A.* **1976**, *73*, 2206; (b) Tweedle, M. F.; Wilson, L. J.; Garcia-Iniquez; Babcock, G. T.; Palmer, G. *J. Biol. Chem.* **1978**, *253*, 8065.
(15) (a) Landrum, J. T.; Reed, C. A.; Hatano, K.; Scheidt, W. R. *J. Am. Chem. Soc.* **1978**, *100*, 3232. (b) Reed, C. A.; Landrum, J. T. *FEBS Lett.* **1979**, *106*, 265.
(16) Kolks, G.; Frihart, C. R.; Coughlin, P. K.; Lippard, S. J. *Inorg. Chem.* **1981**, *20*, 2933.
(17) Kolks, G.; Lippard, S. J., manuscript in preparation.
(18) Ginsburg, A. P.; Cohen, R. L.; Di Salvo, F. J.; West, K. W. *J. Chem. Phys.* **1974**, *60*, 2657.
(19) Krasney, S.; Lilienthal, H. R. IBM Thomas J. Watson Research Center Report RC 5504, 1975.
(20) Selwood, P. W. "Magnetochemistry"; Interscience: New York, 1956.

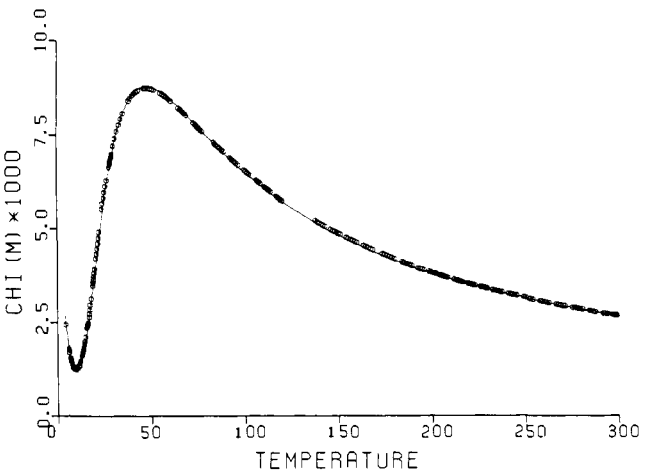

Figure 3. Corrected molar magnetic susceptibility (cm^3 mol^{-1}) vs. absolute temperature for $[Cu(pip)]_2(im)(NO_3)_3 \cdot 2.5H_2O$, **7**. Experimental data are shown as open circles. The solid line shows the least-squares fit to the data using the parameters and equations described in the text.

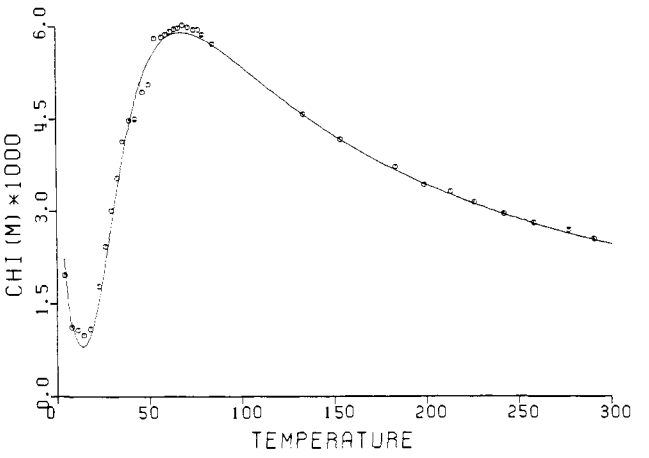

Figure 4. Corrected molar magnetic susceptibility (cm^3 mol^{-1}) vs. absolute temperature for $[Cu(PMDT)]_2(2\text{-MeIm})(ClO_4)_3$, **8**. Experimental data are shown as open circles. The solid line shows the least-squares fit to the data using the parameters and equations described in the text.

Diamagnetic corrections were estimated by using Pascal's constants.[21] The value of -127×10^{-6} cm^3 mol^{-1} used for the pip ligand was obtained from measurements of $Zn(pip)(NO_3)_2$.[16] A value of 60×10^{-6} cm^3 mol^{-1} was assumed for the temperature-independent paramagnetic susceptibility of Cu^{2+}, unless otherwise stated. Least-squares fitting of the theoretical expressions for the magnetic susceptibility to the data was performed on a VAX 11/780 computer using a locally written least-squares program.[22]

Electron spin resonance spectra of the powdered samples were recorded on a Varian E-line X-band spectrometer at room temperature and at liquid-nitrogen temperature. The g values were calibrated against a sample of diphenylpicrylhydrazil ($g = 2.0036$) which was taped to the quartz sample tube.

Results

The Binuclear Complexes. Equation 2 relates χ_g, the measured

$$\chi_M^{corr} = \chi_g M - \chi_{DIA} \quad (2)$$

magnetic susceptibility per gram of compound, to χ_M^{corr}, the magnetic susceptibility per mole of dinuclear complex, corrected for the diamagnetic susceptibility of the complex. M is the molecular weight and χ_{DIA} the molar diamagnetic susceptibility of the complex. Figures 2–6 display χ_M^{corr} as a function of the temperature for compounds **6–10**, respectively. The maxima in the χ_M^{corr} vs. T plots are indicative of antiferromagnetic intracluster

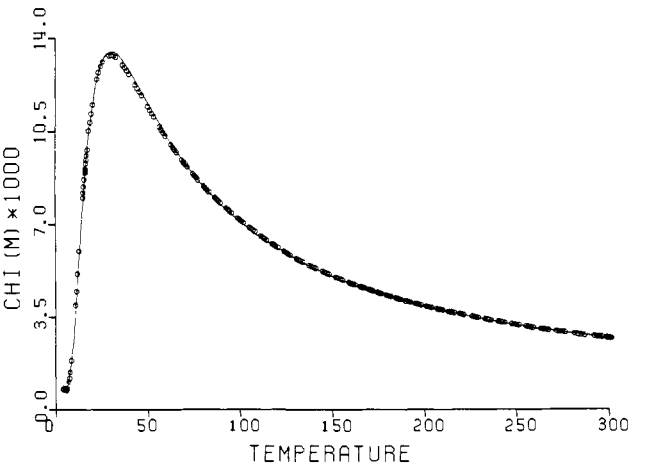

Figure 5. Corrected molar magnetic susceptibility (cm^3 mol^{-1}) vs. absolute temperature for $[Cu(PMDT)]_2(BzIm)(ClO_4)_3 \cdot H_2O$, **9**. Experimental data are shown as open circles. The solid line shows the least-squares fit to the data using the parameters and equations described in the text.

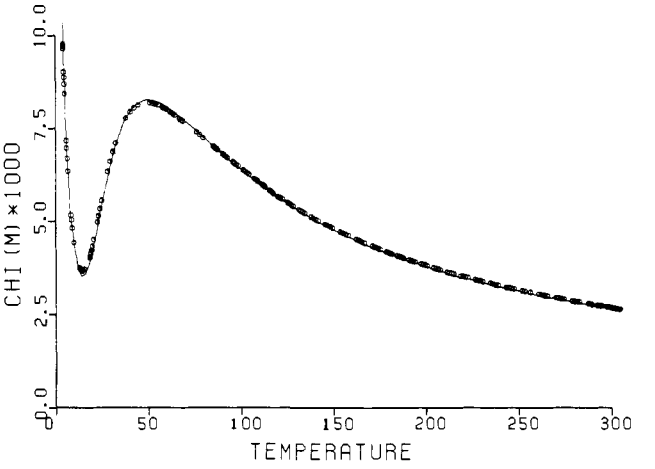

Figure 6. Corrected molar magnetic susceptibility (cm^3 mol^{-1}) vs. absolute temperature for $[Cu(PMDT)]_2(2\text{-MeBzIm})(ClO_4)_3 \cdot MeOH$, **10**. Experimental data are shown as open circles. The solid line shows the least-squares fit to the data using the parameters and equations described in the text.

interactions. The rise in χ_M^{corr} as T decreases at low temperature is due to small amounts of paramagnetic impurities. Values for the coupling constant, J, and the g factor for each of the compounds **6–10** were obtained by fitting eq 3[23] to χ_M^{corr} using all

$$\chi_M^{corr} = \frac{2Ng^2\beta^2}{kT}[3 + \exp(-2J/kT)]^{-1}(1 - p) + p\frac{2Ng^2\beta^2 S(S+1)}{3kT} + \chi_{TIP} \quad (3)$$

of the data from 4.2–300 K. Here p is the mole fraction of paramagnetic impurity. The impurity is assumed to be Cu^{2+} ($S = {}^1/_2$), to have the same diamagnetic correction, molecular weight, and g factor as the binuclear complex, and to have a magnetic susceptibility that follows the Curie law.[2] The other symbols have their usual meaning.

The quantity minimized in the least-squares fitting process was $RMIN \equiv \sum[\chi_M^{corr}(obsd) - \chi_M^{corr}(calcd)]^2$, and each point was given equal weight. As a convenient statistical indicator of the quality of the least-squares fits, we have chosen the generalized R factor,[24] eq 4, with the weights, w, set to unity. Table I lists

$$R = \left[\frac{\sum[\chi_M^{corr}(obsd) - \chi_M^{corr}(calcd)]^2 w}{\sum[\chi_M^{corr}(obsd)]^2 w}\right]^{1/2} \quad (4)$$

(21) Figgis, B. N.; Lewis J. In "Modern Coordination Chemistry"; J. Lewis, J., Wilkins, R. G., Eds.; Interscience: New York, 1960; p 440 ff.
(22) Karlin, K. D. Ph.D. Dissertation, Columbia University, 1975.
(23) Carlin, R. L. *J. Chem. Educ.* **1966**, *43*, 521.

Table I. Parameters Obtained from the Least-Squares Fitting of the Magnetic Susceptibilities[a]

compd[b]	J, cm^{-1}	g	$\langle g \rangle$[c]	N[d]	p[e]	R[f]
$[Cu_2(bpim)(NO_3)_2]ClO_4 \cdot 2H_2O$	−81.8 (5)	2.118 (11)	2.11 (1)	57	0.004	0.0441
$[Cu(pip)]_2(im)(NO_3)_3 \cdot 2.5H_2O$	−26.91 (2)	2.107 (1)	2.11 (1)	243	0.012	0.0098
$[Cu(PMDT)]_2(2\text{-MeIm})(ClO_4)_3$	−38.1 (3)	2.050 (10)	2.09 (1)	36	0.011	0.0333
$[Cu(PMDT)]_2(BzIm)(ClO_4)_3 \cdot H_2O$	−16.99 (1)	2.090 (1)	2.09	203	0.004	0.0103
$[Cu(PMDT)]_2(2\text{-MeBzIm})(ClO_4)_3 \cdot$ MeOH	−29.82 (4)	2.108 (1)	2.09 (1)	193	0.049	0.0104
$[Cu_2(bpim)(im)]_2(NO_3)_4 \cdot 4H_2O$						
$J_1 = J_2, J_3 = 0$	−73.97 (16)	2.221 (3)	2.11 (1)	167[g]	0.004[h]	0.0164[g]
$J_1 \neq J_2, J_3 = 0$	−87.64 (4)[i]	2.132 (1)	2.11 (1)	167[g]	0.004[h]	0.00326[g]
	−35.0 (4)[j]					

[a] Standard deviations, in parentheses, refer to the least significant digit. [b] Formula used in eq 2. [c] Obtained from ESR studies at 77 K. [d] Number of data points collected and used in the least squares refinement. [e] Mole fraction of paramagnetic impurity (see text). [f] Goodness of fit, eq 4. [g] For data above 20 K. [h] p was fixed for all of the fits for this compound. [i] For J_1. [j] For J_2.

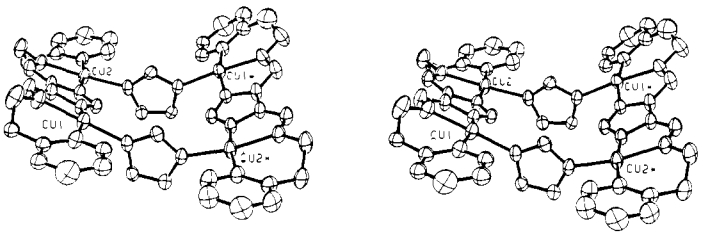

Figure 7. Stereo ORTEP drawing of the $[Cu_2(bpim)(im)]_2^{4+}$ cluster. Starred and unstarred atoms are related to each other by a crystallographically required twofold axis which is perpendicular to and passes through the center of the quadrilateral described by atoms Cu1, Cu2, Cu1*, and Cu2*.

the values of J, g, p, and R obtained from the refinements, and the least-squares curves are shown as the full lines in Figures 2–6. Tables S1–S5 list the observed and calculated values of χ_M^{corr} as a function of temperature.[25] Table I also lists the average g values, $\langle g \rangle$, obtained from the ESR studies of the solids. At both room and liquid-nitrogen temperatures the ESR spectra consist of a broad, nearly isotropic signal at $g \approx 2.1$ and a much weaker, similarly shaped signal at $g \approx 4.2$.

Compounds **6** and **9** have variable compositions; chemical analyses of different batches of crystals suggested that the compounds crystallize with varying amounts of solvent.[16] The parameters reported here are for the particular formulas given in Table I. Least-squares fitting of the data from these compounds was performed by assuming no solvent of crystallization and also with the various combinations of solvent suggested by the chemical analyses. The coupling constant, J, was not affected by these differences, and g^2 was strictly proportional to the assumed molecular weight. Thus for **9**, where analyses suggest the presence of either water, or water and methanol, of crystallization, g^2 varied from 4.277 to 4.528 (4) depending on the formula used but J varied by no more than 0.01 cm^{-1}. The fits were of equal statistical significance.

Because of the small amounts of paramagnetic impurities present and the reasonably large coupling constants of these compounds, inclusion of a Curie term in eq 3 improved the fit of the lowest temperature data points but did not significantly affect the J and g values obtained using only the higher temperature data points.

The Tetranuclear Complex, 5. A stereo ORTEP drawing of the $[Cu_2(bpim)(im)]_2^{4+}$ cation is shown in Figure 7.[10,17] The cation consists of two Cu_2bpim^{3+} units, **6**, bridged by two imidazolate groups. Within each Cu_2bpim unit the Cu···Cu distance is 6.214 (2) Å and the imidzolate ring in the bpim ligand, referred to as the parallel imidazolate ring, lies very nearly in the equatorial copper coordination planes. The Cu···Cu distance between the Cu_2bpim^{3+} units is 5.911 (2) Å and the imidazolate groups that link these units lie almost perpendicular to the copper coordination planes. These imidazolate rings are referred to as the perpendicular imidazolate rings. The two halves of the tetranuclear cluster **5** are related by a crystallographically required twofold axis.

Because of the symmetry of the cluster, only two coupling constants are required as shown in A. It is not possible a priori

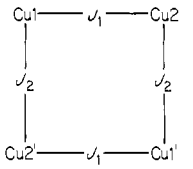

A

to assign the coupling constants to a particular type of imidazolate bridge. Since the Cu1/Cu1′ and Cu2/Cu2′ pairs are not joined by any ligand, the exchange coupling constants $J_{11'}$ and $J_{22'}$ ($\equiv J_3$) have been fixed at zero.

The energy levels resulting from the application of eq 5 were

$$\hat{\mathcal{H}}_{ex} = -2[J_1(\hat{S}_1 \cdot \hat{S}_2 + \hat{S}_{1'} \cdot \hat{S}_{2'}) + J_2(\hat{S}_1 \cdot \hat{S}_{2'} + \hat{S}_2 \cdot \hat{S}_{1'})] \quad (5)$$

obtained from ref 26 and inserted into the Van Vleck equation to obtain eq 6 where $A = J_1 + J_2 + J_3$, $B_i = 2J_i - A$, $B = \sum_{i=1}^{3}$

$$f(J_1,J_2,g,T) = (Ng^2\beta^2/kT)\{[10 \exp(A/kT) + 2B]/ [5 \exp(A/kT) + 3B + \exp[(F - A)/kT] + \exp[-(F + A)/kT]]\} \quad (6)$$

$\exp(B_i/kT)$, and $F = 2(J_1^2 + J_2^2 + J_3^2 - J_1J_2 - J_1J_3 - J_2J_3)^{1/2}$. Although the J_3 term has been set equal to zero for these studies, it has been included in order to present the formula in a compact form. The complete expression for the magnetic susceptibility is eq 7. The term C/T is included to account for the small amount

$$\chi_M^{corr} = f(J_1,J_2,g,T) + C/T + \chi_{TIP} \quad (7)$$

of paramagnetic impurity which is the source of the Curie tail at low temperatures in Figure 8.

Refinement of eq 7 using the data above 40 K gave approximate values for J_1, J_2, and g^2 which indicated that below 20 K the value of $F(J_1,J_2,g,T)$ in eq 7 is zero. Thus, below 20 K eq 7 simplifies to eq 8, and plotting χ_M^{corr} vs. $1/T$ yields C from the slope of the

$$\chi_M^{corr} = C/T + \chi_{TIP} \quad (8)$$

best straight line through the data and χ_{TIP} by extrapolation of

(24) Hamilton, W. C. "Statistics in Physical Science"; The Ronald Press Co.: New York, 1964.
(25) Supplementary material.
(26) Jotham, R. W.; Kettle, S. F. A. *Inorg. Chim. Acta* **1970**, *4*, 145.

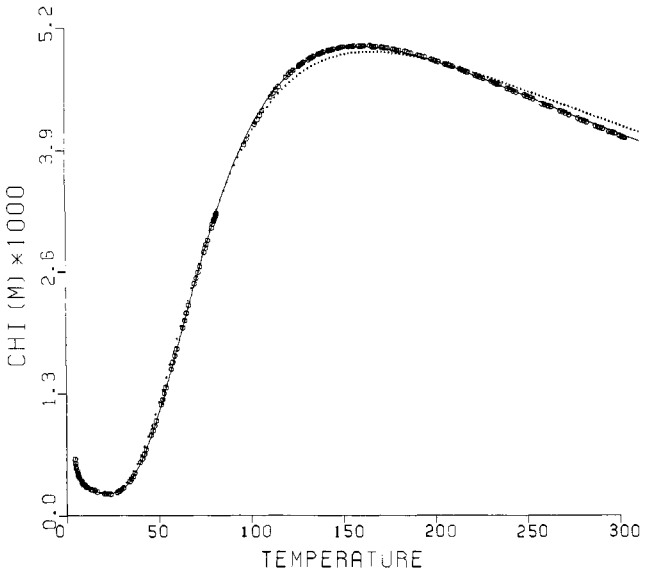

Figure 8. Corrected molar magnetic susceptibility (cm^3 mol^{-1}) vs. absolute temperature for $[Cu_2(bplm)(lm)]_2(NO_3)_4 \cdot H_2O$, **5**. Experimental data are shown as open circles. The solid line is the least-squares curve obtained for the two coupling constant ($J_1 \neq J_2$) model while the dotted line is the least-squares curve obtained for the one coupling constant ($J_1 = J_2$) model using the parameters and equations described in the text.

the data to infinite temperature.[20] This analysis yielded values of 157×10^{-6} cgsu mol^{-1} and 1.56×10^{-3} cgsu K mol^{-1} for χ_{TIP} and C, respectively. The value for C corresponds to 3.8×10^{-3} mole fraction of monomeric Cu^{2+} impurity.

Least-squares fitting of eq 7 using data above 20 K yielded $J_1 = -87.64$ (4) cm^{-1}, $J_2 = -35.0$ (4) cm^{-1}, $g = 2.132$ (1), and $R = 3.26 \times 10^{-3}$. The resulting least-squares curve is shown by the full line in Figure 8. The alternative hypothesis that the coupling between the copper atoms is not a function of the bridging geometry was tested by least-squares fitting of eq 7 to the data above 20 K under the constraint that $J_1 = J_2$, yielding the values $J_1 = J_2 = -73.97$ (16) cm^{-1}, $g = 2.221$ (3), and $R = 16.4 \times 10^{-3}$. This fit is shown as the dotted curve in Figure 8. Evaluation of the ratio $R(J_1 = J_2)/R(J_1 \neq J_2)$ in the usual manner[24] indicates that the model with two different coupling constants is superior to the one coupling constant model at better than the 0.005 level of confidence. Table S6 lists the observed and calculated values of χ_M^{corr}, using both models, as a function of temperature.

The experimentally obtained value of χ_{TIP}, 157×10^{-6} cgsu mol^{-1}, differs from the expected value of 240×10^{-6} cgsu mol^{-1}. This difference probably reflects small systematic errors in determining the diamagnetic correction of the sample bucket and the value of the ferromagnetic correction as well as the usual uncertainty in estimating the diamagnetic correction for the compound. The recommended practice[2] of fixing χ_{TIP} to some estimated value carries with it the tacit assumption that the above corrections are known to much higher accuracy than the measured values of χ_g. Such an assumption is questionable, and its use in the least-squares fitting process[27] can seriously bias the values obtained for the refined parameters. In the case at hand the smaller of the two coupling constants is a very sensitive function of the value chosen for χ_{TIP}. A change of only $\pm 20 \times 10^{-6}$ cm^3 mol^{-1} in the value of χ_{TIP} changes J_1 by ∓ 0.2 cm^{-1} but changes J_2 by ± 1.9 cm^{-1}. After fixing $\chi_{TIP} = 240 \times 10^{-6}$ cm^3 mol^{-1} and determining $C = 1.17 \times 10^{-3}$ cm^3 K mol^{-1}, least-squares fitting of eq 7 to the data above 20 K gave $J_1 = -88.27$ (5) cm^{-1}, $J_2 = -27.8$ (6) cm^{-1}, and $g = 2.094$ (2). The R factor increased to 4.82×10^{-3}, however, indicating a significantly poorer fit. The greater sensitivity of J_2 to the value of TIP seems to be an idiosyncracy of the mathematics and the relative values of J_1 and J_2. Allowing the TIP to vary for the binuclear compounds **7**, **9**, and **10** yields fits to the data which are only slightly better than those obtained by fixing the TIP. The changes in J amount to no more than ± 0.1 cm^{-1}.

Based on earlier studies of a different sample of **5**, we reported[11] values of $J_1 = -87.4$ (1) cm^{-1}, $J_2 = -30$ (1) cm^{-1}, and $g = 2.227$ (7); here χ_{TIP} was fixed at the equivalent of 264×10^{-6} cm^3 mol^{-1}. The high g value as well as our inability to duplicate the data with other samples prompted us to recollect the data on a new sample, the results for which are discussed above. The older data are uniformly ~11% larger than the new data. The source of this error is not known, but any experimental error other than the analytical integrity of the sample, which had been verified, will be compensated for by refining both g^2 and χ_{TIP}, leaving J_1 and J_2 unaffected. Treating the original data as above, we obtain $\chi_{TIP} = 226 \times 10^{-6}$ cm^3 mol^{-1} and $C = 6.23 \times 10^{-3}$ cm^3 K mol^{-1} for data with $T \leq 20$ K and $J_1 = -86.84$ (7) cm^{-1}, $J_2 = -35.2$ (7) cm^{-1}, $g = 2.247$ (2), and $R = 5.19 \times 10^{-3}$. If J_1 is set equal to J_2, we obtain $J = -73.10$ (18) cm^{-1}, $g = 2.334$ (3), and $R = 16.3 \times 10^{-3}$. The agreement of the values for J_1 and J_2 between the two data sets is satisfying. Table S7 lists the observed and calculated values of χ_M^{corr} for this sample.

Discussion

The Spin Exchange Coupling Constant. The six imidazolate-bridged di- and tetranuclear Cu(II) complexes studied all exhibit antiferromagnetic behavior with coupling constants ranging from −17 to −88 cm^{-1}. Structural studies of five of these compounds[10,17,28] show that the closest copper–copper contacts occur within the Cu–im–Cu moiety and range from 5.6 to 6.2 Å. The observed coupling is too large to result from direct, through-space copper–copper interactions; the exchange is therefore mediated by the bridging imidazolate ligands. Compound **5** (Figures 1 and 7) is of particular interest because the coupling constants for the "parallel" and "perpendicular" imidazolate groups are different, −87.64 and −35.0 cm^{-1}, respectively. It is impossible a priori to assign either of these coupling constants to a particular imidazolate group. As shown by X-ray diffraction studies,[10,17,28] however, the dimensions and orientations of the Cu_2im^{3+} moieties in Cu_2bpim^{3+}, **6**, and $[Cu(pip)]_2^{3+}$, **7**, are virtually identical with those of the parallel and perpendicular bridging imidazolate groups, respectively, of $[Cu_2(bpim)(im)]_2^{4+}$, **5**. The coupling constants of −81.8 and −26.9 cm^{-1} observed in **6** and **7**, along with the structural similarty of the corresponding fragments of **5**, **6**, and **7**, permit assignment of the −87.64-cm^{-1} coupling constant to the interaction mediated via the parallel imidazolate groups in **5** and the −35.0-cm^{-1} coupling constant to that mediated via the perpendicular imidazolate groups which link the Cu_2bpim^{3+} halves in **5**. Compound **5** is thus an interesting system requiring two (or more) coupling constants in which (1) the unequivocal assignment of the coupling constants to the particular superexchange pathway has been made on the basis of comparisons with structurally and magnetically isomorphous analogues and (2) the exchange interaction through any one pathway has been shown to be only weakly (a change of from −6 to −8 cm^{-1}) affected by other exchange interactions in the compound.

Table II lists the coupling constants for a variety of imidazolate-bridged copper compounds.[29-40] The value of J is remarkably

(27) Wentworth, W. E. *J. Chem. Educ.* **1965**, *42*, 96.
(28) Dewan, J. C.; Lippard, S. J. *Inorg. Chem.* **1980**, *19*, 2079.
(29) O'Young, C.-L.; Dewan, J. C.; Lilienthal, H. R.; Lippard, S. J. *J. Am. Chem. Soc.* **1978**, *100*, 7291.
(30) Katz, R. N.; Kolks, G.; Lippard, S. J. *Inorg. Chem.* **1980**, *19*, 3845.
(31) Desideri, A.; Cerdonio, M.; Mogno, F.; Vitale, S.; Calabrese, L.; Cocco, D.; Rotilio, G. *FEBS Lett.* **1978**, *89*, 83.
(32) Haddad, M. S.; Hendrickson, D. N. *Inorg. Chem.* **1978**, *17*, 2622.
(33) Haddad, M. S.; Duesler, E. N.; Hendrickson, D. N. *Inorg. Chem.* **1979**, *18*, 141.
(34) Nakao, Y.; Mori, W.; Okuda, N.; Nakahara, A. *Inorg. Chim. Acta* **1979**, *35*, 1.
(35) Mori, W.; Nakahara, A.; Nakao, Y. *Inorg. Chim. Acta* **1979**, *37*, 507.
(36) Nakao, Y.; Mori, W.; Sakurai, T.; Nakahara, A. *Inorg. Chim. Acta* **1981**, *55*, 103.
(37) Suzuki, M.; Kanatomi, H.; Koyama, H.; Murase, I. *Inorg. Chim. Acta* **1980**, *44*, L41.
(38) Hendricks, H. M. J.; Reedjik, J. *Inorg. Chim. Acta* **1979**, *37*, L509.

Table II. Coupling Constants of Some Metal Complexes Bridged by Imidazolate

complex[a]	bridging ligand	$-J$, cm^{-1}	ref
$[Cu_2(bpim)(im)]_2^{4+}$	imidazolate[c]	87.64 (4), 35.0 (4)[d]	e
$Cu_2(bpim)$	imidazolate	81.8 (5)[d]	e
$[Cu(pip)]_2(im)$	imidazolate	26.90 (2)[d]	e
$[Cu(TMDT)]_2(im)$	imidazolate	25.80 (16)[d]	29
$Cu_2(deim)(PMDT)$	imidazolate	45.2 (2)	30
Cu_4BESOD[f]	imidazolate/(histidine)	26	12
cytochrome *c* oxidase	unknown	≥200	13
Cu_2Co_2BESOD[g]	imidazolate(?)	≥300	31
$[Cu(tren)]_2(im)$	imidazolate	38–40	32
$[Cu(Et_5dien)]_2(im)$	imidazolate	20	33
$[Cu(PMDT)]_2(im)$	imidazolate	27	33
$[Cu(dien)]_2(im)$	imidazolate	30	33
$[Cu(dpt)_2(im)$	imidazolate	39	33
$[Cu(Sal{=}Histam)]_4^0$	imidazolate	29.5	34
$[Cu(2\text{-}pyca{=}Histam)]_4^{4+}$	imidazolate	31.3	34
$[Cu(gly\text{-}gly)]_2(im)^{1-}$	imidazolate	19.1	35
$[Cu(gly\text{-}\beta\text{-}ala)]_2im^{1-}$	imidazolate	17.4	36
$[Cu(NS_3Me_3)]_2(im)$	imidazolate	43	37
$[Cu(MNTB)]_2(im)$	imidazolate	30 (4)	38
$[Cu(PMDT)]_2$(2-MeIm)	2-methylimidazolate	38.1[d]	e
$[Cu(tren)]_2$(2-MeIm)	2-methylimidazolate	41,49[h]	32
$[Cu(PMDT)]_2$(BzIm)	benzimidazolate	16.99 (1)[d]	e
$[Cu(PMDT)]_2$(2-MeBzIm)	2-methyl-benzimidazolate	29.82 (4)	e
$[Cu(tren)]_2$(BzIm)	benzimidazolate	22	32
$[Cu(PMDT)]_2$(BiIm)	biimidazolate	<0.5[d]	33
$(Cp_2Ti)_2(BiIm)^0$	biimidazolate	25.2	39
$(Cp_2Ti)_2$(BiBzim)	bibenzimidazolate	19.2	39
$(FeFF)_2(im)^+$	imidazolate	2.3	15a, 40
$MnCo(FF)_2(im)^+$	imidazolate	5	40

[a] Most of the complexes consist of two Cu-L^{2+} units bridged by a polyatomic diamine. The charge of the clusters is 3+ unless noted otherwise. L is a tri- or tetradentate ligand, with the coordinating atoms being nitrogen except for the compound in ref 37. Some abbreviations for the various ligands are TMDT = 1,1,7,7-tetramethyldiethylenetriamine; PMDT = 1,1,4,7,7-pentamethyldiethylenetriamine; dien = diethylenetriamine; dpt = dipropylenetriamine; tren = tris(2-ethylamino)amine; Cp = cyclopentadienyl; FF = face-to-face porphyrin. For other abbreviations, the original references should be consulted. [b] Standard deviations, in parentheses, refer to the last figure quoted. J is defined in eq 1. [c] Contains two different Cu_2im^{3+}-bridging geometries. [d] The structure of this compound is known. [e] This work. [f] The Zn atoms of the active site have been replaced by cupric ion. [g] The Zn atoms of the active site have been partially replaced by Co(II). [h] Two different anions.

constant in compounds of similar bridging ligand and geometry. The compounds $[Cu(pip)]_2(im)(NO_3)_3\cdot 2.5H_2O$, **7**, and $[Cu(PMDT)]_2(im)(ClO_4)_3$ have similar coordination spheres and nearly identical Cu–im–Cu dimensions;[17,29] X-ray studies[17] of **8** and **9** suggest that $[Cu(PMDT)]_2(im)(ClO_4)_3$ would have a very similar geometry. Exchange coupling parameters of −26.9, −25.8,[29] and −27 cm^{-1},[32] respectively, are found for these three compounds.

These results strongly support the suggestion[13] that the J value of −26 cm^{-1} observed in Cu_4BESOD, an active form of bovine erythrocyte superoxide dismutase in which the zinc(II) ions have been replaced by Cu(II) ions, is the result of exchange interactions through a bridging histidine group. The crystal structure of the native enzyme[12] indicates that, in each of the two identical subunits, a copper(II) center is bridged by a histidine imidazolate ring to a zinc(II) ion. In Cu_4BESOD, copper atoms replace zinc atoms in a tetrahedrally distorted environment, as shown by ESR spectroscopy,[12b,13] but this distortion seems to have little effect on the magnitude of the exchange interaction. A form of BESOD

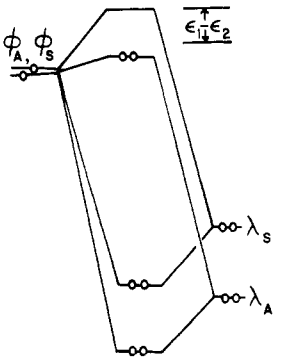

Figure 9. Molecular orbital energy diagram showing the splitting of the mostly metal character antibonding orbitals which can result from the interaction of a pair of Cu(II) orbitals with the orbitals of a bridging ligand (after ref 6).

is also known in which Co(II) ions replace zinc.[31] In analyzing the magnetic properties of this derivative, the authors had to choose between a coupling constant of −8 cm^{-1} and a zero field splitting parameter of ≥600 cm^{-1} or $J \leq -300$ cm^{-1} and a zero field splitting of 15 cm^{-1}. Their choice of the latter set of parameters is highly inconsistent with the results in Table II.

A bridging imidazolate (histidine) ligand between cytochrome a_3 and the ESR silent copper(II) in cytochrome oxidase has been suggested to explain the large ($J \leq -200$ cm^{-1}) coupling observed between the metal centers.[14] The copper compounds reported here have coupling constants of only −88 cm^{-1}, however, and, partly as a result of this discrepancy, the imidazolate-bridged model for cytochrome *c* oxidase has become less fashionable.[15,41,42] A better justification for dismissing the bridging imidazolate model, however, would come from the synthesis and study of an imidazolate-bridged iron porphyrin–copper complex of which none yet exist.

The Mechanism of the Exchange Interaction. When the exchange interactions mediated by the imidazolate group are discussed, the model of ref 6 will be employed. The copper ions have approximately square-planar symmetry with the unpaired electron in a $d_{x^2-y^2}$ orbital. The linear combinations of the two $d_{x^2-y^2}$ orbitals are given by eq 9 and 10, where a and b refer to the two copper

$$\phi_S \approx d^a_{x^2-y^2} + d^b_{x^2-y^2} \quad (9)$$

$$\phi_A \approx d^a_{x^2-y^2} - d^b_{x^2-y^2} \quad (10)$$

atoms. With respect to a mirror plane perpendicular to the imidazolate ring ϕ_S and ϕ_A are symmetric and antisymmetric,

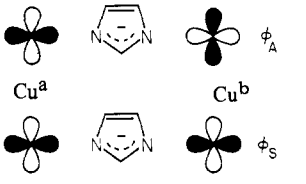

respectively. In the absence of a bridging ligand, ϕ_A and ϕ_S are degenerate in energy. On combining with bridging ligand orbitals (λ_A, λ_S) of proper symmetry, the antibonding orbitals of the resulting species are separated by an energy difference $\epsilon_1 - \epsilon_2$ (Figure 9). It has been shown[6] for a binuclear d^9 complex that $-2J$, the difference between the triplet and singlet states, $E_T - E_S$, is related to $\epsilon_1 - \epsilon_2$ by eq 11, where K_1 and K_2 are nearly constant quantities for small perturbations of the system.

$$-2J = E_T - E_S = -2K_1 + (\epsilon_1 - \epsilon_2)^2/K_2 \quad (11)$$

It has been suggested that both the σ[7,43] and π[7,8] orbitals of nitrogeneous heterocyclic ligands are capable of acting as the

(39) Fieselmann, B. F.; Hendrickson, D. N.; Stucky, G. D. *Inorg. Chem.* **1978**, *17*, 2078.
(40) Landrum, J. T.; Haller, K. J.; Scheidt, W. R.; Reed, C. A. *J. Am. Chem. Soc.* **1981**, *103*, 2640.
(41) Landrum, J. T.; Hatano, K.; Scheidt, W. R.; Reed, C. A. *J. Am. Chem. Soc.* **1980**, *102*, 6729.
(42) Petty, R. H.; Welch, B. R.; Wilson, L. J.; Bottomley, L. A.; Kadish, K. M. *J. Am. Chem. Soc.* **1980**, *102*, 611.
(43) Felthouse, T. R.; Hendrickson, D. N. *Inorg. Chem.* **1978**, *17*, 2636.

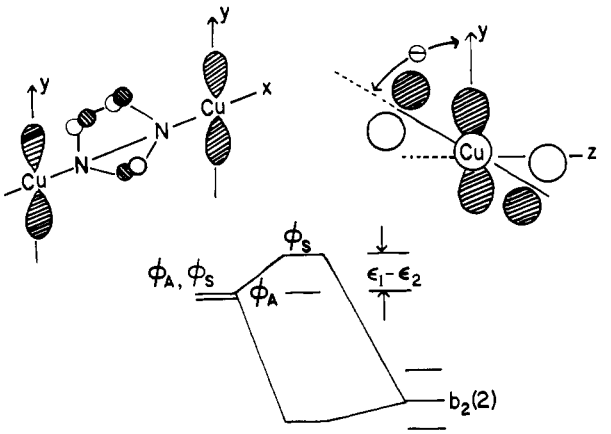

Figure 10. One of the possible π-orbital interactions of the bridging imidazolate ligand and two copper atoms (of b_2 symmetry) showing the angle (θ) between the plane of the bridging imidazolate ligand and the copper coordination plane and the molecular orbital energy level diagram.

superexchange pathways between copper atoms. In the former case two linear combinations of the nitrogen lone pair orbitals, λ_S and λ_A, interact with the metal linear combinations ϕ_S and ϕ_A,

$\lambda_S = LP_1 + LP_2$ $\lambda_A = LP_1 - LP_2$

respectively. Figure 9 shows that the quantity $|\epsilon_1 - \epsilon_2|$ and hence the coupling constant J are somehow proportional to the difference in energy between the two bridging ligand orbitals λ_A and λ_S. Calculations on molecules like **1** and **2** show, and spectroscopic measurements verify, that λ_A lies 1–2 eV or more lower in energy than λ_S and that this energy difference is the result of lone-pair orbital interactions transmitted through the carbon σ orbitals.[44]

In the other superexchange pathway the $d_{x^2-y^2}$ orbitals of the copper atoms may interact with the π orbitals of the imidazolate ion as shown in Figure 10. The angle θ is defined as the dihedral angle between the imidazolate and copper coordination planes. Spatial overlap of the copper $d_{x^2-y^2}$ and the ligand π orbitals is expected to be quite poor compared to the overlap with the imidazolate σ (nitrogen lone pair) orbitals due to the long ($\geq$3 Å) copper–carbon distances. Symmetry mismatch prohibits any copper–nitrogen π interaction. Furthermore, Figure 10 suggests that any $d_{x^2-y^2}$:π orbital overlap should be appreciable only when θ differs considerably from 0 or 90°. In the binuclear compounds **7**, **8**, and **9** the smallest value for θ is 77.4° (average 84.7°)[17] while the corresponding angle in the $Cu_2(bpim)^{3+}$ halves **5**[10,17] and **6**[28] range from only 4.7–13.4°. It is very probable, therefore, that the σ orbitals of the bridging imidazolate groups provide the main, if not the only, superexchange pathways in the compounds reported here.[52]

The σ Exchange Pathway. Correlation with Bridging Ligand pK_a. Coupling constants of −16.99, −26.90, and −38.1 cm^{-1} are observed for the benzimidazolate-, imidazolate-, and 2-methylimidazolate-bridged compounds **7**, **8**, and **9**, respectively. These values are in qualitative agreement with the values observed in a similar series[32] of $[Cu(tren)]_2(im)X_3$ complexes in which the same bridging ions were utilized (−22, −39, and −41 to −49 cm^{-1}, respectively). The differences in exchange coupling mediated by the various bridging ligands in the $Cu(tren)^{2+}$ complexes were postulated to be related to the angle ϕ defined in the drawing.

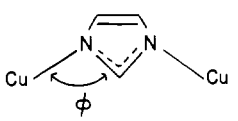

Inclusion of a methyl group at C-2 was expected to increase ϕ due to steric interactions with the $Cu(tren)^{2+}$ groups, thus increasing $|J|$. A decrease in ϕ was expected to be the result of steric interactions between the fused benzene group and the tren ligand with concomitant diminution of $|J|$. None of the compounds had been structurally characterized, however.

Table III. Comparison of the Copper–Imidazolate Geometry, Coupling Constant, and pK_a of the Bridging Imidazolate Group for Compounds 7, 8, and 9

compd	ϕ,[a] deg	$-J$, cm^{-1}	pK_a[b]	ref
$[Cu(PMDT)]_2(BzIm)(ClO_4)_3 \cdot H_2O$	128, 123	17.00 (1)	5.4	*c*
$[Cu(TMDT)]_2(im)(ClO_4)_3$	129, 129	25.80 (16)	6.95	28
$[Cu(pip)]_2(im)(NO_3)_3 \cdot 2.5H_2O$	120, 121, 124, 128	26.91 (2)	6.95	*c*
$[Cu(PMDT)]_2(2\text{-MeIm})(ClO_4)_3$	120.6, 120.6	38.1 (3)	7.75	*c*

[a] See diagram in text. [b] Reference 45. [c] This work.

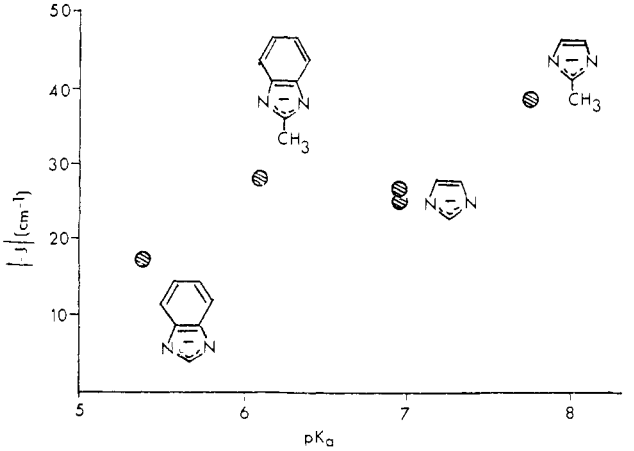

Figure 11. Plot of the observed coupling constants vs. the first pK_a of the bridging ligand for the imidazolate-bridged complexes reported in this thesis. The pK_a's for the imidazolium/imidazole equilibria were taken from ref 45. A similar trend is seen if the imidazole/imidazolate pK_a is used.

Table III shows that no such correlation exists between the coupling constant and the angle ϕ for the compounds reported here. An approximate correlation is observed, however, between the pK_a of the equilibrium $imH_2^+ \rightleftharpoons imH + H^+$ and the coupling constant for the corresponding imidazolate-bridged complex. Figure 11 is a plot of $|J|$ vs. the pK_a[45] of the bridging ligand for compounds **7**, **8**, **9**, and **10**.

It is reasonable that the magnitude of the coupling constant should be proportional to the pK_a's of the neutral form of the bridging ligand whenever the exchange interaction is mediated by a ligand σ-electron pathway. The electronic features that stabilize the N–H bonds of the imidazolium cation will also enhance the interactions between the nitrogen lone pair orbitals of the imidazolate group and the σ-symmetry copper $d_{x^2-y^2}$ orbitals. The strength of a metal–ligand bond, as reflected in the stability constants for the reaction M + L → ML, is directly correlated with ligand basicity (pK_a) as has frequently been observed;[46] and theoretical calculations[47] support this trend. No simple correlation is expected, however, between $|J|$ and the stability constants for copper–imidazole complexes; these values reflect both the basicity (a σ effect) as well as the electron-withdrawing abilities (a π effect) of the ligand.[48]

Hoffmann has shown[6] that a reduction (or increase) of electron density on the donor atoms of the bridging ligand lowers (raises)

(44) Hoffmann, R. *Acc. Chem. Res.* **1970**, *4*, 1.

(45) Bruice, T. G.; Schmir, G. L. *J. Am. Chem. Soc.* **1958**, *80*, 148. The pK_a meant here and throughout this paper refers to the protonated form of the neutral ligand.

(46) Martell, A. E.; Calvin, M. "Chemistry of the Metal Chelate Compounds", Prentice-Hall: Englewood Cliffs, NJ, 1952; p 151.

(47) Bhattacharyya, S. P. *J. Chem. Soc., Dalton Trans.* **1980**, 345.

(48) Sundberg, R. J.; Martin, R. B. *Chem. Rev.* **1974**, *74*, 471.

the energy of the molecular orbitals that contain substantial character of the atoms involved. The methyl group (a σ-donor) in the 2-methylimidazolate ion increases the electron density on the nitrogen atoms of the ligand with respect to the imidazolate ion, thus raising the absolute energy of the linear combination of the lone-pair orbitals. The metal $d_{x^2-y^2}$ and ligand lone pair orbitals are now closer in energy, improving orbital overlap and resulting in an increase in $(\epsilon_1 - \epsilon_2)^2$ and an increase in $|J|$ (Figure 9). The reverse argument applies for the σ-withdrawing, fused benzene ring of the benzimidazolate ion with concomitant diminution of $|J|$. The two effects tend to cancel in the 2-methylbenzimidazolate complex, and in fact a slightly larger coupling constant is observed in this compound than in the imidazolate-bridged complexes. Although the correlation between $|J|$ and the pK_a of the bridging ligand is imperfect, it is perhaps more noteworthy that the *differences* in pK_a's and the coupling constants for any two bridging ligands depend only on their substituent differences.

A correlation between the donor ability of the bridging ligand substituents, σ_R in the language of the Hammett relationship,[49] and the magnitude of magnetic exchange was previously noted for a series of para-substituted pyridine *N*-oxide bridged copper dimers.[50] The variability of the geometries of the OCuOCu moieties, however, prevented an unambiguous statement from being made about the relationship between the donor ability of the substituent and the coupling constant.[4] An attempt to identify a relationship between substituents and coupling in *p*-phenylenediamine-bridged compounds[43] was unsuccessful owing to a correlation between the coupling constants and the counterions used to crystallize the complexes. Surprisingly, no correlation was noted between $|J|$ and the substituent groups for a series of substituted pyrazine bridged polymers $[Cu(pyrazine)(NO_3)_2]_n$,[8] and, partially because of this lack of correlation, a π exchange mechanism was chosen. The present work thus appears to be the first unequivocal, due to the benefit of extensive structural data, demonstration of the predicted relationship between the basicity of the bridging ligand, the σ-donor ability of the substituent groups, and the magnitude of the magnetic exchange mediated by the ligand. The correlation between pK_a and $|J|$ suggests that the much weaker exchange interactions mediated by the σ system of pyrazine ($\sim$3 cm^{-1})[7] may be a result of the much lower pK_a value of this ligand, $\sim$1.

Superexchange in Complexes Bridged by the Chelating Imidazolate Ligands. The values of 81–88 cm^{-1} observed for $|J|$ in the Cu_2bpim^{3+} units of **5** and **6** are much larger than those for the other imidazolate-bridged complexes in Table II. The substituent effect just described would not alone explain such a large $|J|$ value, especially considering the electron-withdrawing nature of the Schiff's base linkages. The larger $|J|$ values are also not explainable by the fact that the relative orientations of the copper coordination and imidazolate ring planes differ between Cu_2bpim^{3+} and the other binuclear complexes. This difference would only affect the superexchange interactions through the imidazolate π-electron system and these interactions are expected to be weak compared to the σ exchange interactions in **7**, **8**, **9**, and **10** (vide supra).

The only remaining possibility is the value for the angle ϕ, as defined previously. In compounds **7**, **8**, and **9**, and in the perpendicular Cu–im–Cu moiety of **5** values of 120–128° are observed[17] for ϕ. In **6**[28] and in the parallel Cu–im–Cu moiety of **5**,[17] however, this angle ranges from 142 to 145° because the Cu^{2+} atom is part of a five-membered chelate ring. It has, in fact, been suggested[32] that an increase in ϕ should cause an increase in $|J|$. CNDO/2 calculations[32] of the imidazolate anion indicate that the highest occupied molecular orbital which could provide a σ exchange pathway for the copper $d_{x^2-y^2}$ orbitals has major contributions from the two nitrogen orbitals shown.

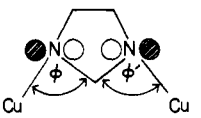

Increasing the angles ϕ and ϕ' improves the overlap between these nitrogen atomic orbitals and the copper $d_{x^2-y^2}$ orbitals thus leading to an increase in $|J|$. $|J|$ should be a maximum when both Cu–N vectors are parallel to the imidazolate carbon-carbon bond.[52]

More detailed justification for expecting $|J|$ to depend on ϕ comes from theoretical calculations[51] on fragment **11**. This moiety

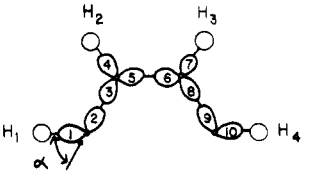

11

is analogous to the N–C–C–N fragment of the imidazolate anion with orbitals 1 and 10 corresponding to the nitrogen lone pair orbitals, LP_1 and LP_2. As stated previously, the difference in energy between the linear combinations (1 + 10) and (1 − 10) is an important factor in determining the value $(\epsilon_1 - \epsilon_2)^2$ (Figure 9) and hence the magnitude of the coupling constant. This difference in energy is the result of the interaction of orbitals 1 and 10 through the σ orbital system of the fragment.[51] The primary source of this interaction is the overlap of the orbitals 1 and 10 with the orbitals 5 and 6, respectively. The magnitude of the overlap of orbitals 1 with 5 (and 6 with 10) is greatest when the two orbitals are trans and parallel to each other, as drawn, and decreases as the angle α decreases. The energy difference between λ_S and λ_A (Figure 9) increases with the angle α, raising the value of $(\epsilon_1 - \epsilon_2)^2$ and, therefore, $|J|$.

The large coupling observed in the Cu_2bpim^{3+} units is consistent with this analysis. Further experimental support for the ϕ dependence of $|J|$ comes from magnetic studies[30] of **12**. This cation

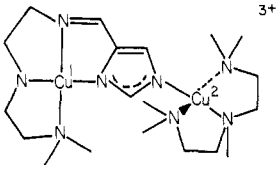

12, $Cu_2(deim)(PMDT)^{3+}$

contains structural features similar to that found both in Cu_2bpim^{3+} and in compounds **7**–**9**. Although the crystal structure of **12** has not been determined, it is likely that its ϕ angles will be similar to those found in **6** and **7**–**9**, namely, $\sim$143° for the Cu1–N bond and $\sim$124° for the Cu2–N bond. A J value between that found in **6** (−82 cm^{-1}) and in **7** (−27 cm^{-1}) is thus predicted. The observed value, −45.2 (2) cm^{-1}, falls in the expected range but differs from the simple average of the coupling constants in **6** and **7**, −54.5 cm^{-1}. No correlation between ϕ and $|J|$ was found for **7**, **8**, or **9**. This result may reflect the small range of ϕ values observed (120–128°), or it may indicate that the dependence of J on ϕ rapidly diminishes as ϕ decreases.

The lone-pair orbitals in the imidazolate ring may also interact with each other through the N–C–N linkage. Calculations show[51] that the energy separation of the linear combinations (1 + 10) and (1 − 10) in fragment **13** below are inexplicably greater than that found for fragment **11**. The relative ordering of the two linear lone pair combinations in **13** is, however, the reverse of that in **11**. The dependence of the energy separation on the relative

(49) Hammett, L. P. "Physical Organic Chemistry"; McGraw-Hill: New York, 1970.

(50) Hatfield, W. E.; Paschal, J. S. *J. Am. Chem. Soc.* **1964**, *86*, 3888. Also see ref 4.

(51) Hoffmann, R.; Imamura, A.; Hehre, W. J. *J. Am. Chem. Soc.* **1968**, *90*, 1499.

(52) **Note Added in Proof**: This conclusion is also supported by the recent report (Matsumoto, K.; Ooi, S.; Nakao, Y.; Mori, W.; Nakahara, A. *J. Chem. Soc., Dalton Trans.* **1981**, 2045) of an imidazolate-bridged dicopper(II) complex having θ values of 5.8° and 10.4°, ϕ = 124°, and J = −19 cm^{-1}.

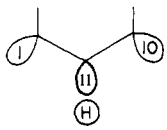

13

orientations of orbitals 1, 11, and 10 has not been investigated.

Although the above discussion has centered on through-bond interaction of the lone-pair orbitals with each other, direct, through-space overlap of these orbitals may occur. Clearly, the overlap is a maximum when the lone-pair orbitals are collinear, as is nearly the case in Cu_2bpim^{3+}, and decreasing ϕ will decrease $|J|$. It is therefore difficult to distinguish between a through-space or through-bond mechanism for the ϕ dependence of $|J|$. Calculations show,[51] however, that the contribution from direct overlap is much smaller than that due to the indirect overlap.

Acknowledgment. This work was supported by Grant No. GM-16449 from the General Medical Institute of the National Institutes of Health.

Registry No. 5, 60881-47-2; **6**, 80010-33-9; **7**, 64254-63-3; **8**, 78003-96-0; **9**, 78003-98-2; **10**, 78018-26-5.

Supplementary Material Available: Tables S1–S7, listing the observed and calculated molar magnetic susceptibilities as a function of temperature for compounds **5–10** (25 pages). Ordering information is given on any current masthead page.

Neighboring Group Participation in Organic Redox Reactions. 5.[1] The Directive and Kinetic Effects of Hydroxyl Groups on Thioether Oxidation

Albert S. Hirschon, Joyce Takahashi Doi,* and W. Kenneth Musker*

Contribution from the Department of Chemistry, University of California, Davis, California 95616. *Received March 30, 1981*

Abstract: Transannular interaction of the hydroxyl group during the aqueous I_2 oxidation of 5-hydroxythiacyclooctane, **2**, 4-hydroxythiacyclohexane, **4**, and 4-hydroxy-4-methylthiacyclohexane, **5**, is indicated by anchimeric assistance, by stereoselection of the trans alcohol–sulfoxide products and by the isolation of the bridged intermediate, 9-oxa-1-thioniabicyclo[3.3.1]nonane triiodide (**1**). In contrast to the behavior of amine thioethers, these reactions are more susceptible to buffer mediation. The two-term rate law indicates that there are two major pathways. Both involve hydroxyl participation and sulfurane intermediates, but one path most likely involves coordination of buffer to sulfur.

Our recent studies of intramolecular catalysis of organic redox reactions revealed that transannular thioether and tertiary amine groups cause dramatic accelerations of the rate of oxidation of thioethers by aqueous I_2.[1,2] A natural extension is the examination of the weakly nucleophilic hydroxyl group and its influence on the reaction mechanism.[3]

Studies of the mechanism of the I_2 oxidation of thioethers in aqueous solution were initiated by Higuchi and Gensch.[4,5] Their method is to monitor the decrease in the I_3^- concentration by its absorption at 353 nm as the reaction proceeds. Additional information about the reaction can be obtained from the retardation of the rate due to iodide inhibition. This information has been used to determine the minimum number of intermediates which must contain iodine atoms prior to the rate-determining step. Structures of many of these and other intermediates have been proposed without adequate characterization. In this study of hydroxyl group participation in the I_2 oxidation of cyclic thioethers we have isolated and determined the structure of an alkoxysulfonium salt intermediate[3] and have confirmed the stereochemistry of the products.

The alkoxysulfonium salt intermediate, 9-oxa-1-thioniabicyclo[3.3.1]nonane triiodide, is the first alkoxysulfonium salt whose crystal structure had been determined. The structures of the sulfoxide products of the reaction buffered at pH 8 or 9 were determined both by independent syntheses and by NMR. These cyclic alcohol–sulfoxides are predominantly (>92%) the isomer in which the hydroxyl and sulfoxide groups are trans.

Since our major interest is in neighboring group participation in the I_2 oxidation of thioethers, the reactions were run under conditions in which buffer involvement would be minimized. Nevertheless, we obtained evidence for a mechanism involving two major paths: one path is buffer dependent and the other path buffer independent. These two paths were then correlated with the iodide dependence. The buffer independent path was found to be inverse first order in iodide: The major buffer dependent path is inverse second order in iodide.

From both kinetic and structural studies we have shown that hydroxyl participation does occur and the intramolecular interaction is manifested in both the kinetics and product stereochemistry. From these results a more definitive mechanism of the I_2 oxidation can be proposed which proceeds via hydroxyl-bridged sulfurane intermediates.

Experimental Section

Kinetic Measurements. Procedures have been described previously.[1,3-5] The absorbance of I_3^- at 353 nm followed the rate law $d[I_3^-]/dt = -[I_3^-][R_2S]k_2$. Values of k_2 in M^{-1} s^{-1} are used in the figures and table. For the slower rates of **3** and of **4** in phosphate buffer, corrections were applied to the absorbances due to a very slow rate of I_3^- loss which was monitored in solutions in the absence of the thioether. Solutions of **2** in water were prepared immediately before they were used at pH 6 or 7. At pH 8 and 9, buffered solutions of **2** were prepared.

Materials. 5-Hydroxythiacyclooctane, **2**,[6] thiacyclooctane, **3**,[7] 4-hydroxythiacyclohexane, **4**,[8] 4-hydroxy-4-methylthiacyclohexane, **5**,[9] were

(1) For paper IV in this series, see Doi, J. T.; Musker, W. K. *J. Am. Chem. Soc.* **1981**, *103*, 1159.
(2) Doi, J. T.; Musker, W. K.; deLeeuw, D. L.; Hirschon, A. S. *J. Org. Chem.* **1981**, *46*, 1239.
(3) Hirschon, A. S.; Beller, J. D.; Olmstead, M. M.; Doi, J. T.; Musker, W. K.; *Tetrahedron Lett.* **1981**, *22*, 1195.
(4) Gensch, K. H.; Higuchi, T. *J. Pharm. Sci.* **1967**, *56*, 177.
(5) (a) Higuchi, T. and Gensch, K.-H. *J. Am. Chem. Soc.* **1966**, *88*, 5486. (b) Gensch, K.-H.; Pitman, I. H.; Higuchi, T. *J. Am. Chem. Soc.* **1968**, *90*, 2096.
(6) 5-Hydroxy-1-thiacyclooctane was obtained by sodium borohydride reduction of 1-thiacyclooctan-5-one in ethanol, using aqueous KOH in the workup.[2]
(7) Mandolini, L.; Vontor, T. *Synth. Commun.* **1979**, *9*, 857.

0002-7863/82/1504-0725$01.25/0